

Electronic Supplementary Information for:

Giant Field Dependence of the Low Temperature Relaxation of the Magnetization in a Dysprosium(III)-DOTA Complex

Pierre-Emmanuel Car, Mauro Perfetti, Matteo Mannini, Annaick Favre, Andrea
Caneschi, and Roberta Sessoli*

*Department of Chemistry 'Ugo Schiff' and INSTM RU, University of Florence,
50019 Sesto Fiorentino, Italy*

1. Synthetic procedures

The reaction was carried out under aerobic conditions. Unless otherwise stated, all reagents were purchased from Sigma-Aldrich and were used as received without further purification.

Synthesis of Na[Dy(DOTA)(H₂O)]·4H₂O:

The compound was prepared following the procedure reported by Desreux^[1] with slight modifications. A mixture of Dy₂O₃ (0.371 mmol), 1,4,7,10-tetraazacyclododecane-N,N',N'',N'''-tetraacetic acid "H₄DOTA" (0.743 mmol) and NaOH (0.743 mmol) in 15 mL of distilled water was heated for few days at 80°C until obtaining a clear solution. After few days, the mixture was cooled to room temperature, centrifugated and filtrated to remove the residual suspension. Single-crystals of Na[Dy(DOTA)(H₂O)]·4H₂O suitable for X-ray diffraction analysis (**Figure S1**), were obtained by a diffusion method^[2] from a water and acetone solution at room temperature.

Synthesis of Na[Y_xDy_{1-x}(DOTA)(H₂O)]·4H₂O:

The Dysprosium complexes were diluted in the diamagnetic host constituted by the isostructural^[3] Yttrium analogues with 20:80 ratio. The synthetic procedure described above was repeated starting from 0.297 mmol of Y₂O₃ and 0.074 mmol of Dy₂O₃. The crystals obtained were analyzed by AES-ICP and the composition was found to be Dy = 4.358 % and Y = 11.24 % in weight. The molecular formula of the compound resulted to be Na[Y_{0.82}Dy_{0.18}(DOTA)(H₂O)]·4H₂O.

2. Crystal structure analysis

A colourless crystal of Na[Dy(DOTA)(H₂O)]·4H₂O was mounted on a glass capillary and transferred to a Oxford Kappa CCD diffractometer. The CrysAlisPro program was used to determine the unit cell parameters and for data collection. The structure was solved by direct methods and refined against F² full-matrix least-squares techniques. Hydrogen atoms were included using Refxyz model (refined H-atom coordinates only). Complete crystallographic data is included in the Crystallographic Information File (CIF).

Crystal data for Na[Dy(DOTA)(H₂O)]·4H₂O: C₁₆H₃₄N₄O₁₃NaDy, *M* = 675.96 g.mol⁻¹, *T* = 293 K, triclinic space group *P*-1 (No. 2), *a* = 8.719(1) Å, *b* = 9.079(1) Å, *c* = 15.637(1) Å, *α* = 82.962(5)°, *β* = 85.824(5)°, *γ* = 81.637(5)°, *V* = 1213.5 Å³, *Z* = 2, diffraction reflexion (°) 4.28 < 2θ < 29.08, ρ_{calcd} = 1.844 g.cm⁻³, μ = 3.168 mm⁻¹, *R*_{int} = 0.0716, *R*₁ = 0.0457, *wR*₂ = 0.0857 for 3855 reflections with *I* > 2σ(*I*) and 316 parameters, *S* = 0.910. CCDC 795879.

Na[Dy(DOTA)(H₂O)]·4H₂O (**Figure S1**) crystallizes in the triclinic *P*-1 space group. The dysprosium ion has a nine coordination number provided by eight donor sites (four oxygen and four nitrogen) in a square antiprismatic geometry, with a water molecule Ow1 capping the O1 O2 O5 O6 plane. The compound is isostructural to the Praseodymium, Neodymium, Europium, Gadolinium, Holmium, Lutetium complexes with a twist angle of 39.3(1)° in agreement with what found for the other members of the isostructural series. The average Dy-O and Dy-N bond distances (**Table S1**) of 2.330 (4) Å and 2.642 (5) Å, respectively, are in good agreement with the other members of the isostructural series and with the other reported Dy-DOTA complex of formula Na[Dy(DOTA)(H₂O)]·NaOH·7H₂O.^[4,5]

Table S1: Selected structural parameters for Na[Dy(DOTA)(H₂O)]·4H₂O.

Dy-N (Å)	Dy-O (Å)	Dy-Ow (Å)	Na-O (Å)
2.621(4)→2.667(5)	2.321(4)→2.340(5)	2.466(4)	2.313(5)→2.551(5)

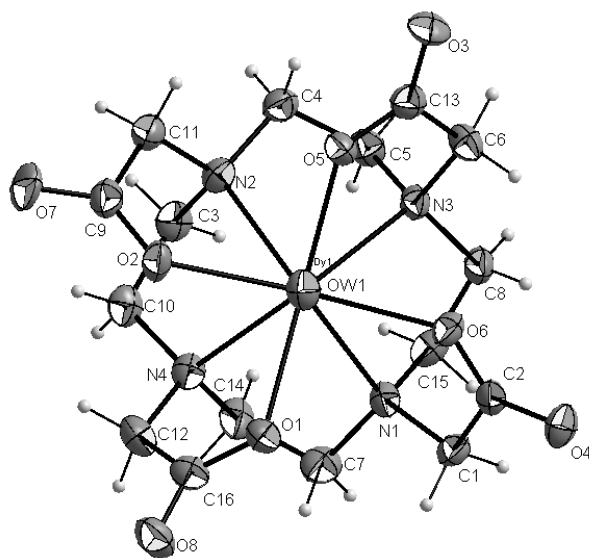


Figure S1: Structure of the anionic part $[\text{Dy}(\text{DOTA})(\text{H}_2\text{O})]^-$. Displacement ellipsoids are drawn at the 40% probability level.

The exclusive presence of the crystallographic phase described above in the batch of crystals used for the magnetic characterization was confirmed by recording the x-ray diffraction pattern (see Fig. S2) with a Bruker AXS D8 advance X-ray diffractometer.

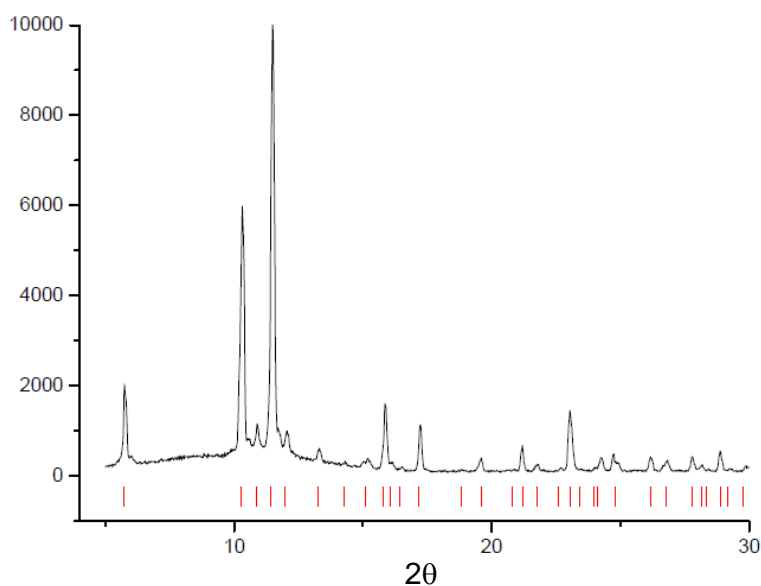


Figure S2. X-ray diffraction pattern of $\text{Na}[\text{Dy}(\text{DOTA})(\text{H}_2\text{O})]\cdot 4\text{H}_2\text{O}$ obtained with $\text{Cu K}\alpha$ radiation. Red sticks correspond to the calculated principal peaks ($I/I_{\text{max}} > 5\%$).

3. Magnetic characterization

Dc magnetic measurements were performed by using a Quantum Design MPMS SQUID magnetometer on 35.5 mg of microcrystalline $\text{Na}[\text{Dy}(\text{DOTA})(\text{H}_2\text{O})]\cdot 4\text{H}_2\text{O}$ pressed in a pellet to avoid field induced orientation of the crystallites.

Ac susceptibility was measured using the same instrumentation for the frequency range 0.07 - 1000 Hz, and with a home-made inductive probe adapted to a Oxford Instruments Maglab2000 platform for the frequency range 0.1-70 kHz.

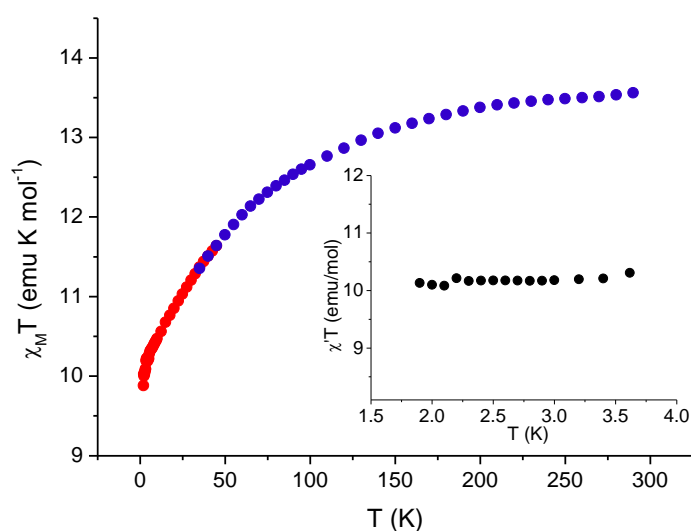


Figure S3. Temperature dependence of the χT product of $\text{Na}[\text{Dy}(\text{DOTA})(\text{H}_2\text{O})]\cdot 4\text{H}_2\text{O}$ measured at 1000 Oe (red points) below $T = 50$ K and at 10000 Oe (blue points) above $T = 35$ K. In the inset low frequency $\chi' T$ observed at low temperature, zero static field and 1 Hz frequency of the oscillating field.

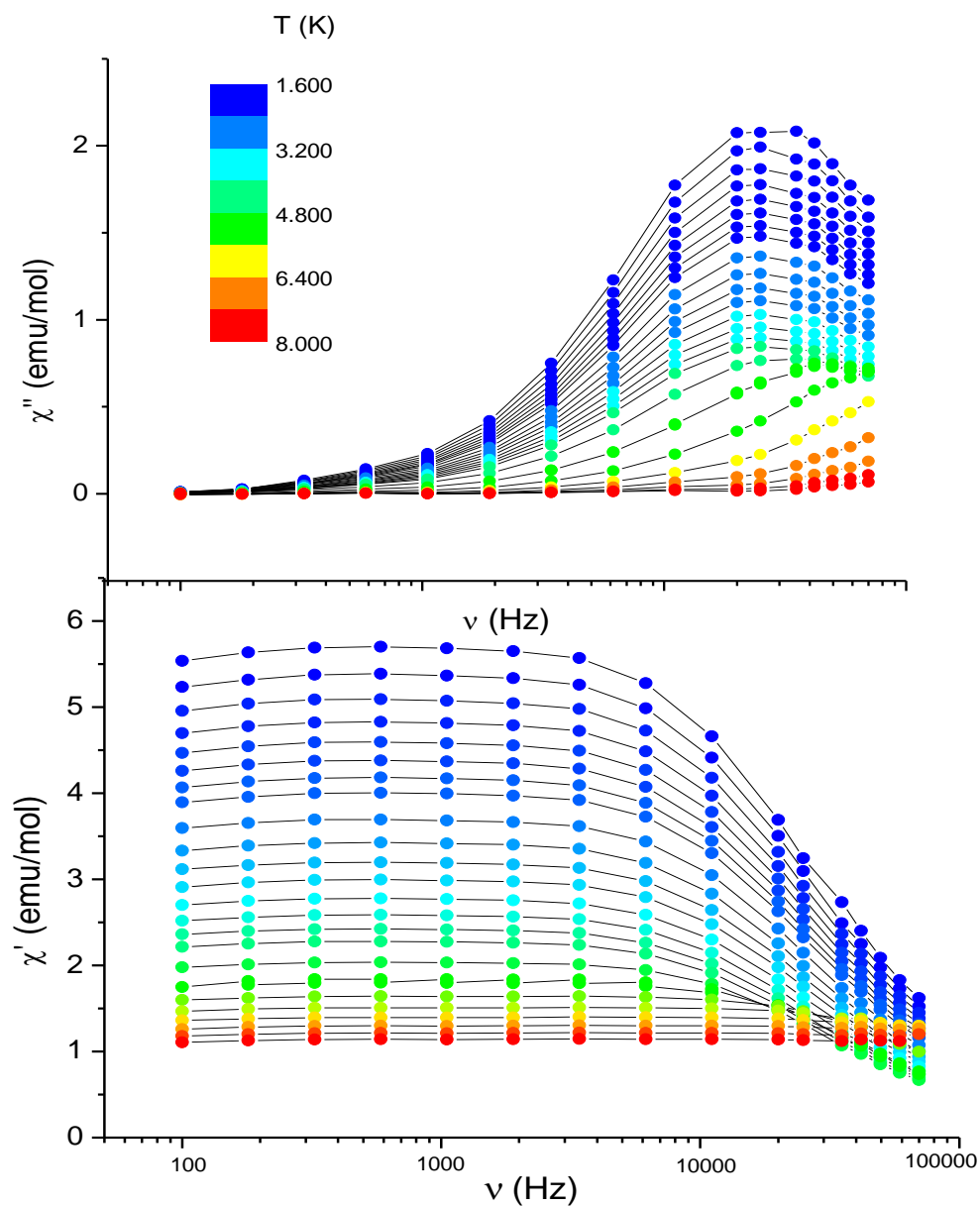


Figure S4. Frequency dependence of the imaginary (top) and real (bottom) components of the *ac* susceptibility of Na[Dy(DOTA)(H₂O)]·4H₂O measured in zero static field in the temperature range 1.8 – 8 K (temperature color scale in the legend).

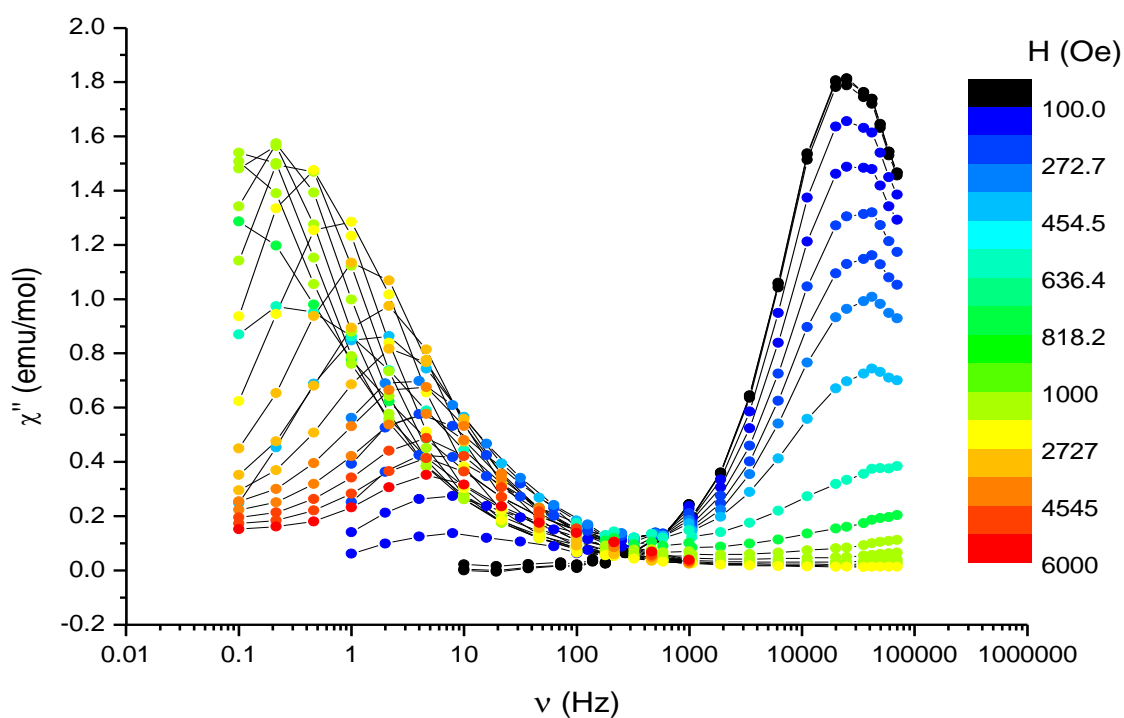


Figure S5. Plot of the imaginary component of the *ac* susceptibility of Na[Dy(DOTA)(H₂O)]·4H₂O against frequency at 1.8 K and variable static fields up to 6000 Oe (field color scale in the legend).

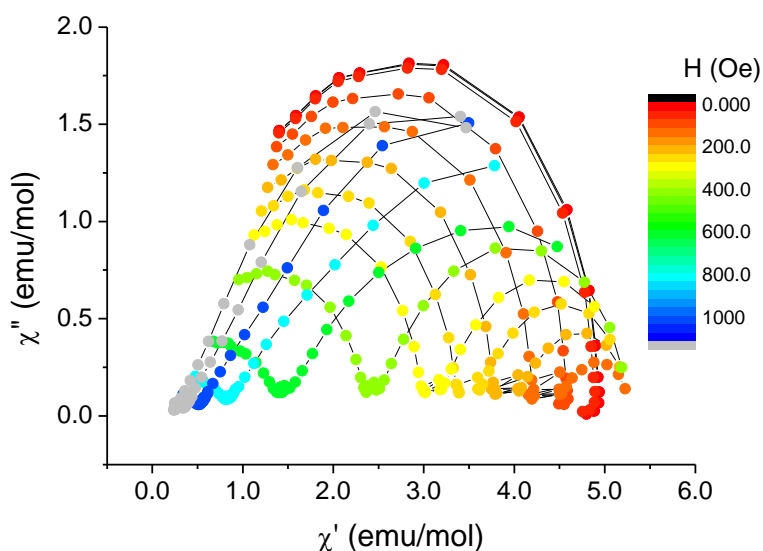


Figure S6. Cole-Cole plots, deduced from the *ac* susceptibility of Na[Dy(DOTA)(H₂O)]·4H₂O against frequency at 1.8 K, are reported for variable static fields up to 1200 Oe (field color scale in the legend). Two semicircles are evident for fields in the range 100 – 800 Oe.

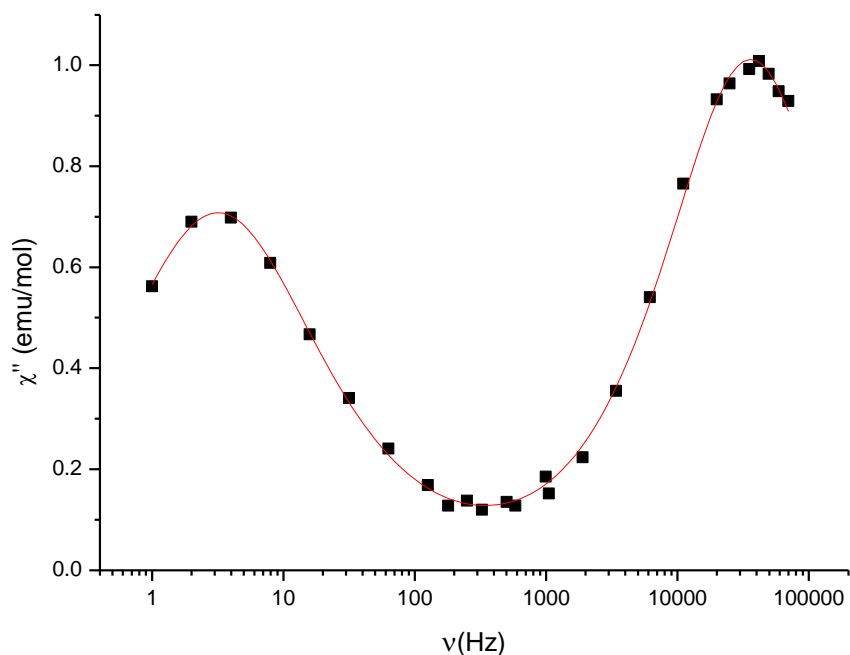


Figure S7. Representative example of the fitting of χ'' data versus frequency at intermediate field ($H_{dc}=300$ Oe) using a function that is the sum of two Casimir and Du Pre's functions:

$$\Gamma = (\chi_T - \chi_S)_A \frac{(\omega\tau_A)^{1-\alpha_A} \cos(\pi \frac{\alpha_A}{2})}{1 + 2(\omega\tau_A)^{1-\alpha_A} \sin(\pi \frac{\alpha_A}{2}) + (\omega\tau_A)^{2-2\alpha_A}} + (\chi_T - \chi_S)_B \frac{(\omega\tau_B)^{1-\alpha_B} \cos(\pi \frac{\alpha_B}{2})}{1 + 2(\omega\tau_B)^{1-\alpha_B} \sin(\pi \frac{\alpha_B}{2}) + (\omega\tau_B)^{2-2\alpha_B}}$$

The best fit parameters are: $(\chi_T - \chi_S)_A = 2.24(4)$ emu/mol, $\tau_A = 5.02(2) \times 10^2$ ms, $\alpha_A = 0.28(1)$, $(\chi_T - \chi_S)_B = 2.74(4)$ emu/mol, $\tau_B = 4.4(1) \times 10^{-3}$ ms, and $\alpha_B = 0.19(1)$, for the slow and fast relaxing species, respectively.

Table S2. Relaxation times extracted for the fast (B) and slow (A) relaxation processes as a function of the applied static field at $T= 1.8$ K.

Field (kOe)	τ_B (ms)	τ_A (ms)
0.00	5.93	<i>n.d.</i>
0.02	5.91	<i>n.d.</i>
0.04	5.88	<i>n.d.</i>
0.10	5.61	2.18E+04
0.15	5.27	2.36E+04
0.20	4.95	2.88E+04
0.25	4.65	3.71E+04
0.30	4.39	5.04E+04
0.40	3.88	8.85E+04
0.60	2.11	5.07E+05
0.80	0.75	3.86E+06
1.00	<i>n.d.</i>	5.16E+06
1.20	<i>n.d.</i>	2.30E+06
1.40	<i>n.d.</i>	1.12E+06
1.60	<i>n.d.</i>	7.32E+05
1.80	<i>n.d.</i>	5.18E+05
2.00	<i>n.d.</i>	3.79E+05
2.40	<i>n.d.</i>	2.20E+05
2.80	<i>n.d.</i>	1.39E+05
3.20	<i>n.d.</i>	9.56E+04
3.60	<i>n.d.</i>	7.14E+04
4.00	<i>n.d.</i>	5.76E+04
4.40	<i>n.d.</i>	4.92E+04
4.80	<i>n.d.</i>	4.39E+04
5.20	<i>n.d.</i>	4.06E+04
5.60	<i>n.d.</i>	3.76E+04

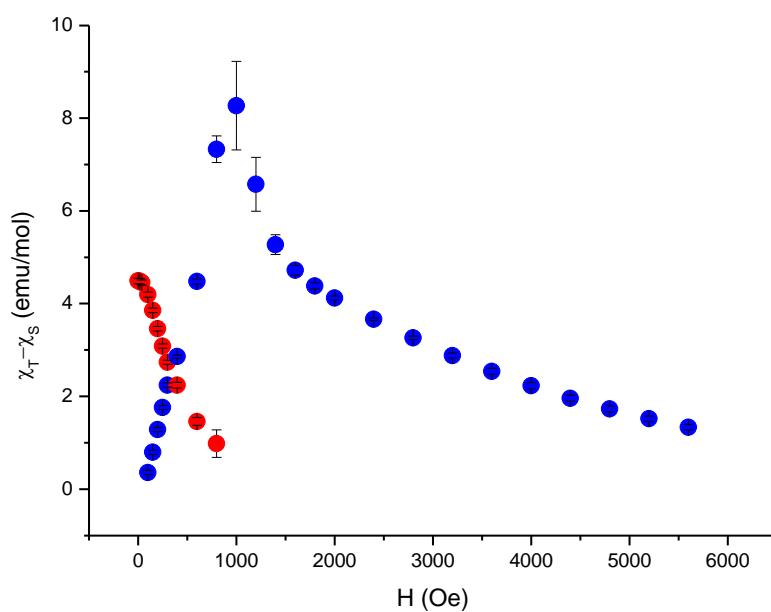


Figure S8. Difference between isothermal and adiabatic susceptibility ($\chi_T - \chi_S$) against field for the fast (red) and slow (blue) processes extracted from the fitting of the χ'' vs. frequency curves as shown in Fig. S6.

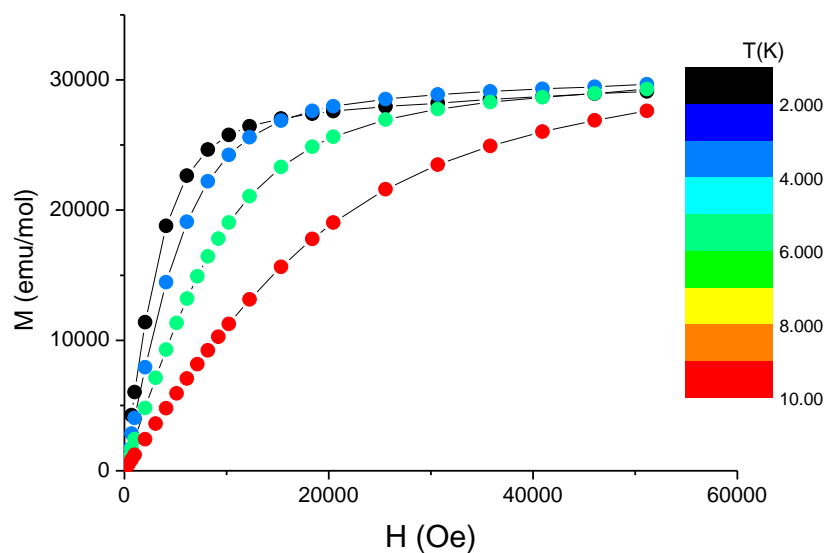


Figure S9. Molar magnetization versus field of $\text{Na}[\text{Dy}(\text{DOTA})(\text{H}_2\text{O})] \cdot 4\text{H}_2\text{O}$ at various temperatures.

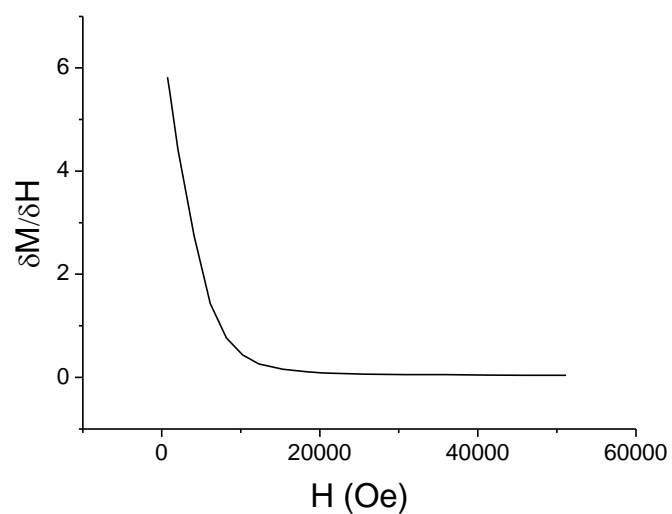


Figure S10. Derivative of the magnetization curve of Na[Dy(DOTA)(H₂O)]·4H₂O at $T = 1.8$ K used to estimate the isothermal susceptibility, i. e. $\chi'(v \rightarrow 0)$.

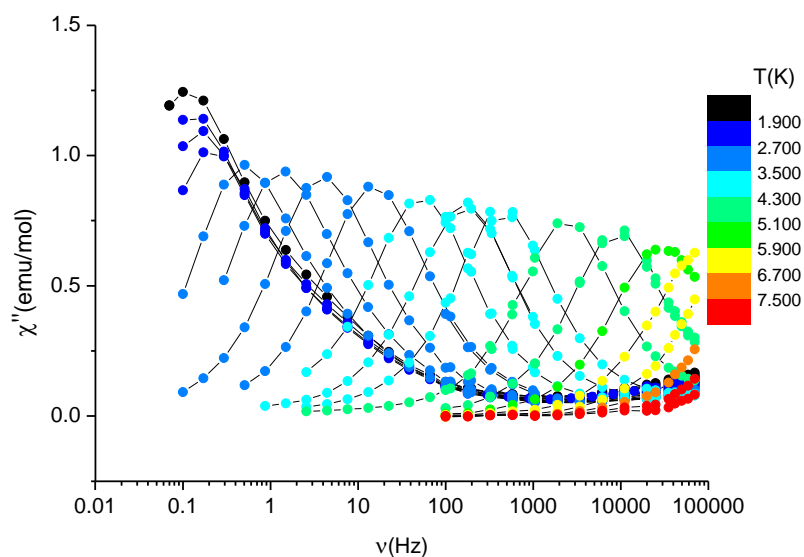


Figure S11. Frequency dependence of the imaginary component of the *ac* susceptibility of Na[Dy(DOTA)(H₂O)]·4H₂O measured at $H_{dc} = 900$ Oe and several temperatures (temperature color scale in the legend).

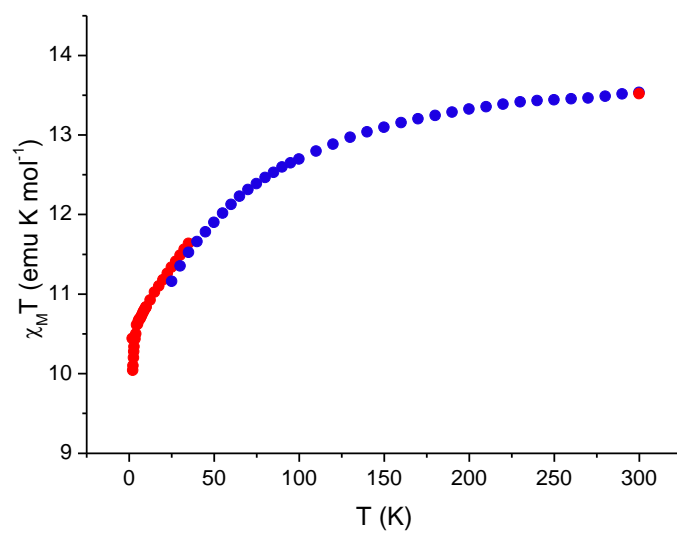


Figure S12. Temperature dependence of the χT product of $\text{Na}[\text{Y}_{0.82}\text{Dy}_{0.18}(\text{DOTA})(\text{H}_2\text{O})]\cdot 4\text{H}_2\text{O}$ measured at 1000 Oe (red points) below $T = 40$ K and at 10000 Oe (blue points) above $T = 25$ K.

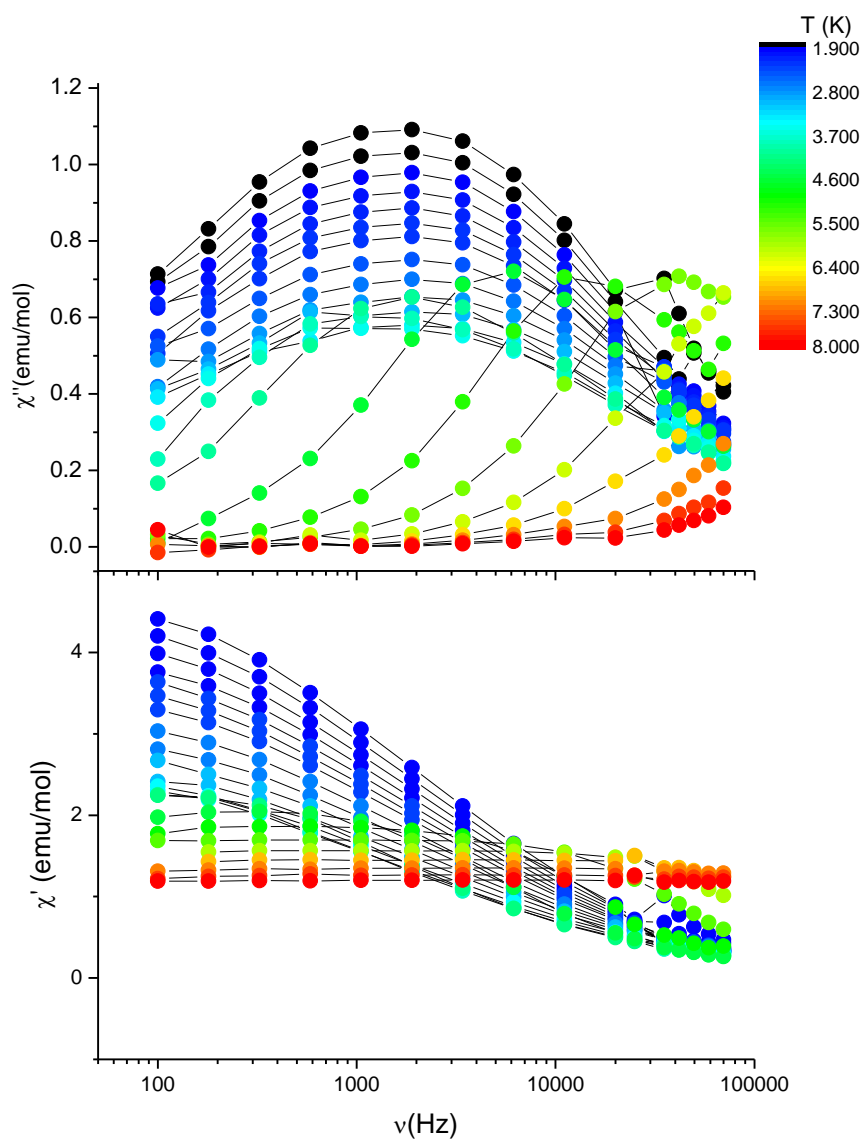


Figure S13. Frequency dependence of the imaginary (top) and real (bottom) components of the *ac* susceptibility of $\text{Na}[\text{Y}_{0.82}\text{Dy}_{0.18}(\text{DOTA})(\text{H}_2\text{O})]\cdot 4\text{H}_2\text{O}$ measured in zero static field in the temperature range 1.8 – 8 K (temperature color scale in the legend).

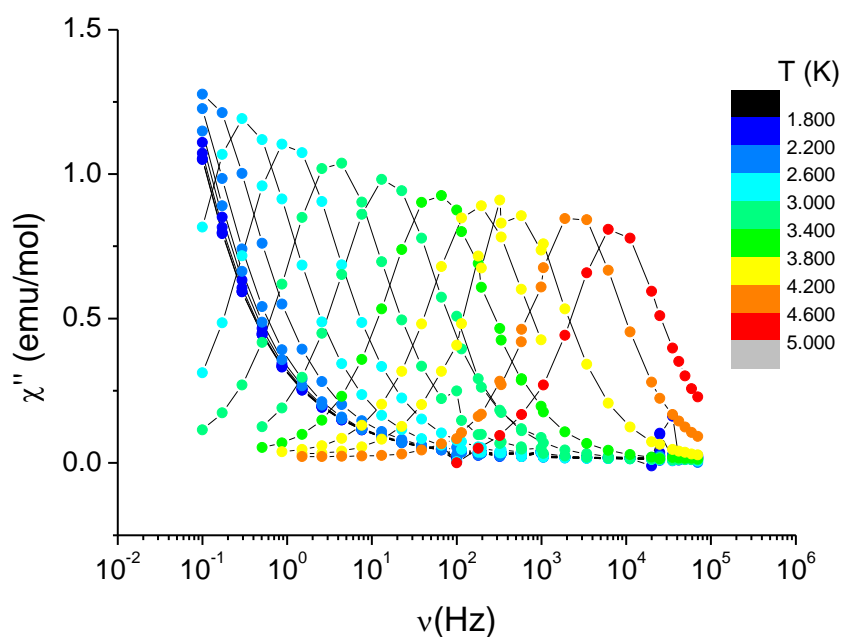


Figure S14. Frequency dependence of the imaginary component of the *ac* susceptibility of $\text{Na}[\text{Y}_{0.82}\text{Dy}_{0.18}(\text{DOTA})(\text{H}_2\text{O})]\cdot 4\text{H}_2\text{O}$ measured at $H_{ac} = 900$ Oe and several temperatures (temperature color scale in the legend).

[1] J. F. Desreux, *Inorg. Chem.*, **1980**, *19*, 1319.

[2] F. Benetollo, G. Bombieri, S. Aime, M. Botta, *Acta Cryst.*, **1999**, *C55*, 353.

[3] Viola-Villegas, N.; Doyle, R.-P. *Coord. Chem. Rev.*, **2009**, *253*, 1906.

[4] P. Vojtisek, P. Cigler, J. Kotek, J. Rudovsky, P. Hermann, I. Lukes, *Inorg. Chem.*, **2005**, *44*, 5591.

[5] G. Bombieri, R. Artali, *J. Alloy. Comp.*, **2002**, *344*, 9.